JOURNAL OF BACTERIOLOGY, May 2007, p. 3547–3555 Vol. 189, No. 9
0021-9193/07/$08.00+0 doi:10.1128/JB.00093-07
Copyright © 2007, American Society for Microbiology. All Rights Reserved.

Assembly of Fimbrial Structures in *Pseudomonas aeruginosa*: Functionality and Specificity of Chaperone-Usher Machineries[▽]

Ségolène Ruer, Silke Stender, Alain Filloux,* and Sophie de Bentzmann

Laboratoire d'Ingénierie des Systèmes Macromoléculaires, CNRS-IBSM-UPR9027, 31 Chemin Joseph Aiguier, 13402 Marseille Cedex 20, France

Received 17 January 2007/Accepted 1 February 2007

Fimbrial or nonfimbrial adhesins assembled by the bacterial chaperone-usher pathway have been demonstrated to play a key role in pathogenesis. Such an assembly mechanism has been exemplified in uropathogenic *Escherichia coli* strains with the Pap and the Fim systems. In *Pseudomonas aeruginosa*, three gene clusters (*cupA*, *cupB*, and *cupC*) encoding *c*haperone-*u*sher *p*athway components have been identified in the genome sequence of the PAO1 strain. The Cup systems differ from the Pap or Fim systems, since they obviously lack numbers of genes encoding fimbrial subunits. Nevertheless, the CupA system has been demonstrated to be involved in biofilm formation on solid surfaces, whereas the role of the CupB and CupC systems in biofilm formation could not be clearly elucidated. Moreover, these gene clusters were described as poorly expressed under standard laboratory conditions. The *cupB* and *cupC* clusters are directly under the control of a two-component regulatory system designated RocA1/S1/R. In this study, we revealed that Roc1-dependent induction of the *cupB* and *cupC* genes resulted in a high level of biofilm formation, with CupB and CupC acting with synergy in clustering bacteria for microcolony formation. Very importantly, this phenotype was associated with the assembly of cell surface fimbriae visualized by electron microscopy. Finally, we observed that the CupB and CupC systems are specialized in the assembly of their own fimbrial subunits and are not exchangeable.

Formation and maturation of biofilm in *Pseudomonas aeruginosa* are now well documented at the molecular level and involve a large arsenal of cell surface-associated organelles, including flagella (19, 25) and type IVa (19, 25) or type IVb (4) pili. More recently, putative fimbrial structures, called Cup for *c*haperone-*u*sher *p*athway, have been identified from the *P. aeruginosa* genome sequence (36). The chaperone-usher pathway is a conserved process for assembling fimbriae at the surfaces of gram-negative bacteria (28, 30, 32, 35) and involves an outer membrane protein, the usher, a periplasmic chaperone, and a fimbrial subunit (28, 35). Fimbrial subunits entering the periplasm via the Sec system are bound by the chaperone and form a soluble complex. The chaperone plays a critical role in folding, stabilizing, and capping the subunit prior to polymerization into a fiber. Chaperone–fimbrial-subunit complexes are targeted to the oligomeric, pore-forming, outer membrane usher (6, 33). Assembly of fimbrial subunits into fibers is then processed by donor strand exchange (3), which leads to the growth of the fimbriae through the usher from the tip to the base (27). Finally, fimbrial structures assembled by the chaperone-usher pathway have frequently been reported as having a role in bacterial pathogenesis (14), facilitating bacterial attachment to host tissue and promoting biofilm formation (23, 30).

Three gene clusters have been identified in the *P. aeruginosa* genome (31) and named *cup* (36). The *cupA*, *cupB*, and *cupC* gene clusters encode an usher, a chaperone, and at least one fimbrial subunit (8). The major fimbrial subunits were named CupA1, CupB1, and CupC1; the chaperones were named CupA2, CupB2, and CupC2 and belonged to the FGS chaperone subfamily (30), for which the F1-G1 loop length is short in comparison with the one of the FGL subfamily (15); and the usher proteins were named CupA3, CupB3, and CupC3 (Fig. 1). While the CupC system is restricted to these three components, the *cupA* cluster comprises two additional genes coding for an additional chaperone, CupA5, and a protein of 453 residues, CupA4, which might be an atypical adhesin, even though it does not clearly show the two-domain organization found in the PapG (7, 22) and FimH (2) adhesins. The *cupB* cluster also contains an additional chaperone, CupB4, and a typical two-domain adhesin, CupB6. The *P. aeruginosa cup* gene clusters thus look different from the *pap* or *fim* gene clusters, with, for example, multiple chaperone-encoding genes. In this respect, the *P. aeruginosa cup* gene clusters are similar to the *caf1* gene cluster of *Yersinia pestis* (9) or to the *hif* gene cluster of *Haemophilus influenzae* (10). The *cup* gene clusters of genes were described as poorly expressed under laboratory conditions (37) and are regulated by a complex regulatory network involving the HNS-like protein MvaT, acting in a phase-variable manner (38) as a transcriptional repressor for *cupA* (37) and, to a lesser extent, for *cupB* and *cupC* (37). A two-component regulatory system, namely, the RocS1 (the *s*ensor of the Roc1 [*r*egulation *o*f *c*up 1] system)-RocR-RocA1 system, homologous to the BvgS-BvgR-BvgA system of *Bordetella pertussis* (26, 39), which controls a number of virulence factors in this bacterium (13), has recently been identified as controlling *cupB* and *cupC* gene cluster expression (20). The overproduction of the regulator RocA1 or the sensor RocS1 is sufficient to observe the overexpression of *cupB-lacZ* and *cupC-lacZ* transcriptional fusions.

* Corresponding author. Mailing address: Laboratoire d'Ingénierie des Systèmes Macromoléculaires, CNRS-IBSM-UPR9027, 31 Chemin Joseph Aiguier, 13402 Marseille Cedex 20, France. Phone: 33 49 1164127. Fax: 33 49 1712124. E-mail: filloux@ibsm.cnrs-mrs.fr.

▽ Published ahead of print on 9 February 2007.

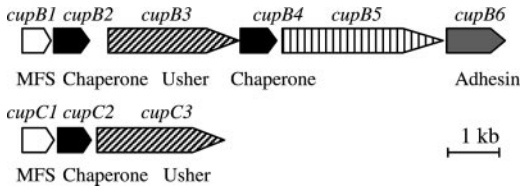

FIG. 1. Genetic organization of the *P. aeruginosa cupB* and *cupC* gene clusters. The *cup* genes are represented with pointed ends indicating the transcriptional orientation. Genes with identical functions are represented with similarly sized and shaded symbols. MFS, major fimbrial subunit.

The structure of chaperone-usher-assembled fibers is morphologically heterogeneous, ranging in form from thick pilus rods that can be polar or can radiate outward from the bacterial cell wall to more flexible and thin fibrillae (5, 9, 16, 18). However, until now, despite the increasing data suggesting the involvement of the *P. aeruginosa* CupA machinery in biofilm formation (12, 36), particularly through autoaggregative behavior (3), there are no studies that could demonstrate the assembly of fimbrial structures by the *P. aeruginosa* Cup machineries.

Taking advantage of the positive role of the sensor RocS1 in the expression of the *cupB-lacZ* and *cupC-lacZ* transcriptional fusions, the present study investigated the specific assembly of CupB and CupC fimbriae at the *P. aeruginosa* cell surface and their subsequent impact in terms of biofilm formation.

MATERIALS AND METHODS

Bacterial strains and growth conditions. The strains and plasmids used in this study are listed in Table 1. Strains were grown at 30°C or 37°C in solid agar M63 medium supplemented with 0.4% L-arginine and 1 mM $MgSO_4$ in the presence of IPTG (isopropyl-β-D-thiogalactopyranoside) at 100 μM or 1 mM for complementation experiments. The *Escherichia coli* TG1 strain was used for standard genetic manipulations. Recombinant plasmids were introduced into *P. aeruginosa* using the conjugative properties of pRK2013. Transconjugants were selected on *Pseudomonas* isolation agar (Difco Laboratories) supplemented with appropriate antibiotics. The following antibiotics at the indicated concentrations were used: for *E. coli*, ampicillin (50 μg/ml), gentamicin (Gm; 25 μg/ml), kanamycin (Km; 25 μg/ml), tetracycline (Tc; 15 μg/ml), and streptomycin (Sm; 50 μg/ml), and for *P. aeruginosa*, carbenicillin (300 μg/ml), Gm (80 μg/ml), Tc (200 μg/ml), and Sm (2 mg/ml).

Construction of *P. aeruginosa* deletion mutants. PCR was used to generate a 550-bp DNA fragment upstream of the *cupC3*, *cupB3*, and *cupB1* genes with the DelC3Up5/DelC3Up3, DelB3Up5/DelB3Up3, and DelB1Up5/DelB1Up3 oligonucleotide pairs, respectively (Table 2). A 550-bp DNA fragment downstream of the *cupC3*, *cupB3*, and *cupB1* genes was PCR amplified using the DelC3Dn5/DelC3Dn3, DelB3Dn5/DelB3Dn3, and DelB1Dn5/DelB1Dn3 oligonucleotide pairs, respectively (Table 2). The resulting DNA fragments were further used as templates for overlapping PCR runs using the external oligonucleotide pairs DelC3Up5/DelC3Dn3, DelB3Up5/DelB3Dn3, and DelB1Up5/DelB1Dn3, respectively, thus leading to a final 1.1-kb DNA fragment that was cloned into the pCR2.1 vector. The resulting DNA fragment bearing appropriate sites, namely, ApaI/SpeI for *cupC3*, SpeI/NsiI for *cupB3*, and BamHI/EcoRV for *cupB1*, was further hydrolyzed and cloned into the suicide vector pKNG101. The recombinant plasmid was then mobilized into *P. aeruginosa*, and the deletion mutants were selected on LB plates containing 5% sucrose and appropriate antibiotics as previously described (17).

Cloning of the *cupB3* and *cupC3* genes. The *cupB3* and *cupC3* genes were amplified by PCR with the oligonucleotides CupB3U and CupB3D or CupC3U and CupC3D, respectively. The genes were cloned into the pCR2.1 vector. The

TABLE 1. Strains and plasmids used in this study[a]

Strain or plasmid	Relevant characteristic(s)	Source or reference
Strains		
E. coli		
TG1	*supE* Δ(*lac-proAB*) *thi hsdR*Δ*5* (F′ *traD36 rpoA*$^+$*B*$^+$ *lacI*^{q}*Z*Δ*M15*)	Lab collection
TOP10F′	F′ [*lacI*^{q} Tn*10*(Tet^r)] *mrcA* Δ(*mrr-hsdRMS-mcrBC*) ϕ80*lacZ*Δ*M15* Δ*lacX74 recA1*	Invitrogen
CC118(λ*pir*)	Host strain for pKNG101 replication, Δ(*ara-leu*) *araD* Δ*lacX74 galE galK phoA20 thi-1 rpsE rpoB argE*(Am) *recA1* Rf^r (λ*pir*)	Lab collection
P. aeruginosa		
PAO1	Wild type	Lab collection
PAO1Δ*pilA*Δ*fliC*	PAO1 mutant with deletions in the *pilA* and *fliC* genes	Lab collection
PAO1Δ*fliC*	PAO1 mutant with a deletion in the *fliC* gene	Lab collection
PAO1Δ*pilA*	PAO1 mutant with a deletion in the *pilA* gene	Lab collection
PAO1Δ*pilA*Δ*fliC*Δ*cupC3*	PAO1 mutant with deletions in the *pilA*, *fliC*, and *cupC3* genes	This study
PAO1Δ*pilA*Δ*fliC*Δ*cupB3*	PAO1 mutant with deletions in the *pilA*, *fliC*, and *cupB3* genes	This study
PAO1Δ*pilA*Δ*fliC*Δ*cupB1*	PAO1 mutant with deletions in the *pilA*, *fliC*, and *cupB1* genes	This study
PAO1Δ*pilA*Δ*fliC*Δ*cupB3*Δ*cupC3*	PAO1 mutant with deletions in the *pilA*, *fliC*, *cupB3*, and *cupC3* genes	This study
PAK	Wild type	Lab collection
PAK*cupB3*::Cb^r	PAK strain with an insertion in the *cupB3* gene	36
PAK*cupC3*::Cb^r	PAK strain with an insertion in the *cupC3* gene	36
Plasmids		
pCR2.1	TA cloning vector for PCR products, *lacZ*α ColE1 f1 *ori* Ap^r Km^r	Invitrogen
pMMB67EH	Broad-host-range vector, IncQ P*tac lacZ*α Gm^r	20
pBBR1MCS-3	Broad-host-range vector, Tc^r	Lab collection
pKNG101	Suicide vector in *P. aeruginosa sacB* Sm^r	Lab collection
pDEST42	Destination vector for gateway technology, T7 promoter, Ap^r	Invitrogen
pBBR*cupC3*	*cupC3* gene cloned in pBBR1MCS-3, Tc^r	This study
pBBR*cupB3*	*cupB3* gene cloned in pBBR1MCS-3, Tc^r	This study
pRK2013	ColE1 *ori tra*$^+$ *mob*$^+$ Km^r	Lab collection
pMMB*rocS1*	*rocS1* gene cloned in pMMB67EH, Gm^r	20
pDEST42-*cupC1*	*cupC1* gene cloned in pDEST42, Ap^r	This study

[a] Cb, carbenicillin; Ap, ampicillin; Tet, tetracycline; Rf, rifampin.

TABLE 2. Oligonucleotides used for mutation engineering and gene cloning

Mutation or complementation	Oligonucleotide (5′→3′)
Mutations	
cupC3	
DelC3Up5	TGT TTC AAG GGG AAG GCT TGC CGA GC
DelC3Up3	TGA CAT TTC ATA TGG CCA CGC GAA TAT TCC
DelC3Dn5	CGT GGC CAT ATG AAA TGT CAC CGC TGC AGT
DelC3Dn3	GTA GCC AGG GAC GAT GCC TTT CTG GTC G
cupB3	
DelB3Up5	CCG CTT CCG TCA GAT ACG AAG
DelB3Up3	CGC CCG GGC ACC GCG GGC GCC TGC GG
DelB3Dn5	TGC CCG GGC GCT GGG GCA ACG AGC CGC
DelB3Dn3	CCG GTA TGG CGA AGC TGG AG
cupB1	
DelB1Up5	GACCGGATGGTTGATAGGTCG
DelB1Up3	CGCCCCGGGCTGATTTCCTTTGGAGTTGTGG
DelB1Dn5	CAGCCCGGGGCGGCGGTCGACGGACGAA
DelB1Dn3	TGGGCGGAACTTCCAGGATATT
Complementations	
cupC3	
CupC3U	TCAGAAGAGCAGAGCAGAGCAG
CupC3D	GTAGCCAGGGACGATGCCTTTCTGGTC
cupB3	
CupB3U	GCCGGTACCCGCGCCATTCTCGACCGA
CupB3D	GCTCTAGACGGTCACAGCGTGCG

cupB3 and *cupC3* genes were subcloned into the broad-host-range vector pBBR1MCS-3 at the restriction enzyme sites KpnI/XbaI and SpeI/XhoI, respectively.

Production of antibodies directed against CupC1. A strategy for antigenic-peptide-based antibody production was used (Eurogentec, Belgium). Two peptides in CupC1, TVKLKFDPVSGTGID and LNSNTEKDGEGNDIT, were selected and synthesized. Two rabbits were inoculated with the designed peptides at a concentration of 200 μg/ml. The immunization protocol included a first injection of the peptide, followed by three boosters at 15 days, 1 month, and 2 months following the original injection. After that period, rabbits were bled. Collected sera were further purified against the initial antigenic peptides. Preimmune sera of the two rabbits were also checked for the absence of cross-reactivity with *P. aeruginosa* whole-cell extracts. Serum specificity was tested on whole-cell extracts of *E. coli* TG1 strains transformed with the pDEST42 vector containing the *cupC1* gene (pDEST42-*cupC1*). The *cupC1* gene was obtained from a comprehensive *P. aeruginosa* gene collection (21), cloned into an entry vector of the Gateway system (Invitrogen), and further moved into a pDEST42 destination vector by L and R lambda phage-specific recombination sites according to the manufacturer's instructions.

Shearing experiments. Bacteria were scraped from plates, and the equivalent of 5 optical density at 600 nm (OD_{600}) units was resuspended in L broth. Shearing was performed by gentle agitation at 4°C overnight. Bacteria were harvested by centrifugation, and the supernatant was further ultracentrifuged at 17,600 × *g* for 10 min at 4°C. The supernatant was then subjected to a first ammonium sulfate (AS) precipitation at a concentration of 50% for 1 h at room temperature and centrifuged at 70,400 × *g* for 45 min at 4°C. The resulting pellet was resuspended in a 500-μl volume of Tris (10 mM, pH 8), whereas the supernatant was subjected to a second AS precipitation at a concentration of 55% and processed as previously described. A protease inhibitor cocktail (Boehringer Mannheim) was added to these different appendage preparations to minimize proteolytic degradation during the procedure.

SDS-PAGE and Western blot analysis. Bacteria were scraped from agar plates containing appropriate antibiotics and IPTG and resuspended in L broth. Finally, the cell extract (or the sheared fraction [SF]) was adjusted to an amount equivalent to a 0.025 OD_{600} unit per μl in a sodium dodecyl sulfate-polyacrylamide gel electrophoresis (SDS-PAGE) loading buffer. The samples were boiled for 10 min and the proteins separated by electrophoresis on a 12% polyacrylamide gel. The proteins were either stained with Coomassie blue or blotted onto nitrocellulose membranes. The CupC1 protein was immunodetected using the CupC1 rabbit polyclonal antibodies at a dilution of 1:1,000. A peroxidase-conjugated goat anti-rabbit immunoglobulin G (Jackson Laboratories) at a dilution of 1:5,000 in Tris-buffered saline containing 10% milk and 0.1% Tween 20 was further applied, and the presence of the protein was revealed using a chemoluminescence revelation kit (Pierce). To check for cytoplasmic and periplasmic leakages during appendage preparation, immunoblotting was performed to detect the cytoplasmic ornithine carbamoyltransferase (OTCase) protein using a specific antibody (a gift from Dieter Haas, Université de Lausanne, Switzerland) at a dilution of 1:500 and the periplasmic thiol-disulfide interchange protein (DsbA) using a specific antibody (a gift from Karl E. Jaeger, IMET, Jülich, Germany) at a dilution of 1:10,000. In the latter case, specific rabbit polyclonal antibodies directed against these proteins were used.

Transmission electron microscopy. Bacterial cells, obtained with growth conditions similar to those described for the shearing experiments, were processed for transmission electron microscopy. The cells were scraped from plates and collected in an Eppendorf tube containing 50 μl of 10 mM phosphate-buffered saline (PBS). A drop of the bacterial suspension was placed on Formvar- and carbon-coated copper grids and left for 5 min. The grids were further fixed with 1% paraformaldehyde for 5 min and rinsed two times with 10 mM PBS for 5 min. For CupC fimbriae detection, grids were further incubated with a 5% bovine serum albumin (BSA) solution in 10 mM PBS for 10 min and incubated with the CupC1 antibodies at a 1:100 dilution in 0.5% BSA and 10 mM PBS for 45 min. The grids were finally incubated with a colloidal solution of conjugated protein A-gold particles (7- or 10-nm diameter) for 30 min in 0.5% BSA, 10 mM PBS. After repetitive washes in 10 mM PBS and in water, grids were immersed in a drop of 1% uranyl acetate for 1 min and were examined in a JEOL 1200EX transmission electron microscope operating at 80.0 kV.

Mass spectrometry. Proteins were cut out from Coomassie blue-stained gels and subjected to procedures routinely performed by the proteomic platform at the IBSM (http://www.ibsm.cnrs-mrs.fr/ifrc/servtech/seq). Briefly, samples were treated via reduction and alkylation processes, digested with trypsin, desalted, and subjected to matrix-assisted laser desorption ionization–time of flight (MALDI-TOF) mass spectrometry analysis. Internal scale-up was done with ions coming from trypsin autolysis and from keratin. Mass values were compared with theoretical values from peptides referenced in databases.

Biofilm formation on inert surfaces. The bacterial adherence assay was performed with 24-well polystyrene microtiter dishes as previously described (36). Bacteria were grown in M63 medium supplemented with 0.4% L-arginine and 1 mM $MgSO_4$ in the presence of IPTG under static conditions at 30°C. Attached bacteria were stained with 100 μl of 1% crystal violet for 15 min and washed twice with water. Stain was extracted by treatment with 400 μl 95% ethanol. Subsequently, 600 μl water was added, and OD_{570} values were measured. All quantification assays were made in triplicate. Alternatively, coverslips were partially immersed in Falcon tubes containing the same medium and further processed for epifluorescence or confocal microscopy.

Epifluorescence and confocal microscopies. Prior to observation, coverslips were fixed with 4% paraformaldehyde and stained using 4′,6′-diamidino-2-phenylindole (DAPI) for 15 min. Slides were observed using an epifluorescence microscope at a ×63 magnification. The number of isolated bacteria was evaluated in the PAO1Δ*pilA*Δ*fliC*Δ*cupB3* and PAO1Δ*pilA*Δ*fliC*Δ*cupC3* mutants in six independent and randomly chosen microscopic fields within the air-liquid interface area. Slides were also observed using an Olympus FV-1000 microscope with a laser diode for excitation at 405 nm. Images were captured and processed by using Fluoview and Amarys software.

RESULTS AND DISCUSSION

Biofilm formation upon RocS1 overproduction. In order to study the role of the putative CupB and CupC fimbriae in biofilm formation, we used a *P. aeruginosa* strain devoid of type IVa pili and of flagella (PAO1Δ*pilA*Δ*fliC*). By eliminating the contribution of these appendages to the biofilm phenotype, we aimed at unraveling the role of other determinants, such as the CupB and CupC fimbriae. It was previously shown that RocS1 overproduction induced the expression of *cupB-lacZ* and *cupC-lacZ* transcriptional fusion (20). In this study, RocS1 was overproduced by introduction of the plasmid pMMB67EH carrying the *rocS1* gene, pMMB*rocS1*, into the PAO1Δ*pilA*Δ*fliC* strain. In pMMB*rocS1*, the *rocS1* gene was placed under the control of the IPTG-inducible *tac* promoter. We then used a

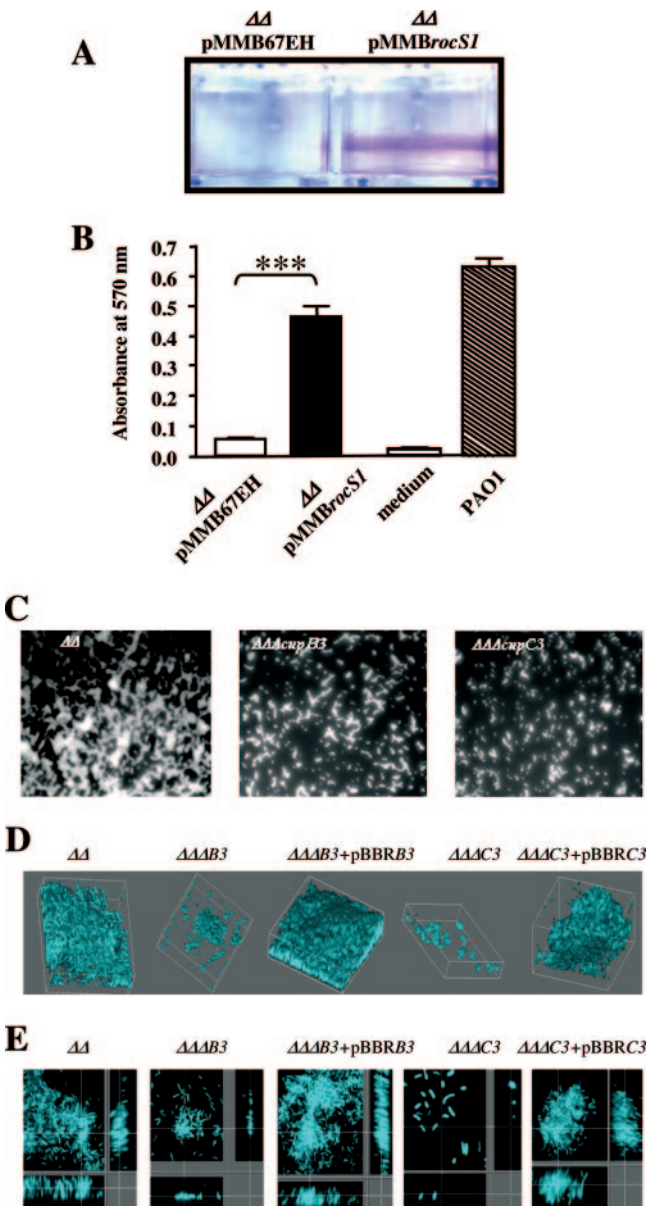

FIG. 2. Biofilm formation by *P. aeruginosa* upon RocS1 overproduction. Strains PAO1Δ*pilA*Δ*fliC*/pMMB*rocS1* and PAO1Δ*pilA*Δ*fliC*/pMMB67EH were inoculated into microtiter plates. (A) After ITPG induction for 48 h at 30°C, bacterial rings that formed at the air-liquid interface were observed by crystal violet staining. (B) The amount of bacteria was quantified after extraction of crystal violet and OD_{570} measurements. Wells inoculated with sterile medium and with the PAO1 strain were also included as controls. ***, $P < 0.001$. (C) Biofilm formation at the air-liquid interface of glass slides immersed in culture medium was analyzed with the PAO1Δ*pilA*Δ*fliC*/pMMB*rocS1* (ΔΔ), PAO1Δ*pilA*Δ*fliC*Δ*cupB3*/pMMB*rocS1* (ΔΔΔ*cupB3*), and PAO1Δ*pilA*Δ*fliC*Δ*cupB3*/pMMB*rocS1* (ΔΔΔ*cupC3*) strains using DAPI staining and epifluorescence microscopic observation at a ×63 magnification. (D) Stacked confocal scanning laser microscopy images of biofilms of the PAO1Δ*pilA*Δ*fliC*/pMMB*rocS1* (ΔΔ), PAO1Δ*pilA*Δ*fliC*Δ*cupB3*/pMMB*rocS1* (ΔΔΔ*cupB3*), and PAO1Δ*pilA*Δ*fliC*Δ*cupB3*/pMMB*rocS1* (ΔΔΔ*cupC3*) strains and of the *trans*-complemented strains with the *cupB3* (ΔΔΔ*cupB3* + pBBR*B3*) and *cupC3* (ΔΔΔ*cupC3* + pBBR*C3*) genes. DAPI was used for staining, and confocal-microscopic observation was done at a ×180 magnification using z slices of 300 nm. (E) Corresponding extracted z images and their respective *xy* and *xz* planes showing biofilms formed by the PAO1Δ*pilA*Δ*fliC*/pMMB*rocS1* (ΔΔ), PAO1Δ*pilA*Δ*fliC*Δ*cupB3*/pMMB*rocS1* (ΔΔΔ*cupB3*), and PAO1Δ*pilA*Δ*fliC*Δ*cupB3*/pMMB*rocS1* (ΔΔΔ*cupC3*) strains and by the *trans*-complemented strains with the *cupB3* (ΔΔΔ*cupB3* + pBBR*B3*) and *cupC3* (ΔΔΔ*cupC3* + pBBR*C3*) genes.

standard biofilm assay with bacteria grown in wells of microtiter plates and biofilm formed at the air-liquid interface stained with crystal violet (see Materials and Methods). Upon IPTG induction and after 48 h of growth, the strain containing pMMB*rocS1* formed a visible biofilm, unlike the corresponding strain containing the empty vector (Fig. 2A). An increase by 10-fold in the amount of attached bacteria was evaluated after crystal violet extraction and quantification (Fig. 2B). We further tested whether the RocS1-dependent overexpression of *cupB* or *cupC* could be linked to the increased biofilm phenotype. We engineered mutations in the usher-encoding genes *cupB3* and *cupC3* using the PAO1Δ*pilA*Δ*fliC* strain. In these mutant strains, PAO1Δ*pilA*Δ*fliC*Δ*cupB3* and PAO1Δ*pilA*Δ*fliC*Δ*cupC3*, we introduced the pMMB*rocS1* plasmid. Coverslips were partially immersed in culture medium containing the parental strain or each of these mutants, and biofilm formation was observed at the air-liquid interface using epifluorescence microscopy (see Materials and Methods). Under these conditions, the parental strain formed dense clusters of cells with hardly any identifiable isolated bacteria (Fig. 2C). The *cupB3* mutant (PAO1Δ*pilA*Δ*fliC*Δ*cupB3*) formed clusters of bacterial cells whose size was considerably reduced, whereas sparse and isolated bacteria were observed between these clusters. For the *cupC3* mutant (PAO1Δ*pilA*Δ*fliC*Δ*cupC3*), the size of the bacterial cell clusters was even more reduced and isolated bacteria were more abundant than with the *cupB3* mutant. This observation was even more obvious when z slices were made through the biofilm using confocal microscopy (Fig. 2D and E). Whereas microcolonies that had acquired a three-dimensional architecture could be readily observed in the parental strain, PAO1Δ*pilA*Δ*fliC*, using stacked z series (Fig. 2D) or extracted z images and their respective *xy* and *xz* planes (Fig. 2E), they were clearly absent in the *cupB3* and *cupC3* mutants. The biofilm formed by these mutants contained only one cell layer, unlike with the parental strain (Fig. 2E, *xy* and *xz* planes, compare the ΔΔΔ*B3* and ΔΔΔ*C3* images to the ΔΔ image). Moreover, isolated bacteria are easily distinguishable in the *cupB3* and *cupC3* mutants (Fig. 2E, *z* images, compare the ΔΔΔ*B3* and ΔΔΔ*C3* images to the ΔΔ image). Importantly, the biofilm phenotype could be restored to the parental level when the corresponding usher genes cloned into pBBRMCS-3 (pBBR*cupB3* or pBBR*cupC3*) were introduced in *trans* (Fig. 2E, images labeled ΔΔΔ*B3* + pBBR*B3* and ΔΔΔ*C3* + pBBR*C3*).

Our results thus confirmed that overexpression of *rocS1* in *trans*, which leads to *cupB* and *cupC* gene expression (20), favored biofilm formation. Our data further revealed that both the CupB and CupC systems play an important role in this process, particularly through bacterial clustering and microcolony formation (Fig. 2C through E). Detailed analysis of the observed biofilm phenotypes suggested that the CupC system appeared to have the more significant contribution, at least in the absence of appendages such as type IVa pili and flagella (25). Indeed, the deletion of *cupC3* resulted in a nearly com-

plete failure to form bacterial aggregates (Fig. 2D and E, lanes ΔΔΔ*C3*), whereas *trans*-complementation by overexpression of *cupC3* resulted in a strong aggregative phenotype (Fig. 2D and E, lanes ΔΔΔ*C3* + pBBR*C3*). In a previous study, the strongest effect in facilitating interbacterial binding and the structuralization of the bacterial community was ascribed to the *cupB* cluster in the *P. aeruginosa* PAK strain (20). However, we showed here that the lack of either the *cupB3* or the *cupC3* gene is sufficient to produce a defect in biofilm formation. Overall, our observations are in favor of a synergy between the CupB and CupC systems, and it is a possibility that the proper architecture of the biofilm might need the simultaneous contributions of both systems. Such a possibility is likely if we consider that both systems are simultaneously controlled by the Roc1 system (20).

If the CupB and CupC systems are involved in the architecture of the bacterial community during biofilm formation, it is a possibility that they act through the assembly of fimbrial structures that favor cell-cell interaction.

Detection of the CupC1 fimbrial subunit upon RocS1 overproduction. The plasmid pMMB67EH and its derivative carrying the *rocS1* gene, pMMB*rocS1*, were introduced into the *P. aeruginosa* strain PAO1Δ*pilA*Δ*fliC*. The bacterial strains were grown on plates and scraped off them, and cell extracts were further processed for analysis by SDS-PAGE (see Materials and Methods). No obvious differences between the Coomassie blue-stained protein profiles of whole-cell extracts obtained from PAO1Δ*pilA*Δ*fliC*/pMMB67EH (Fig. 3A, lane 1) and PAO1Δ*pilA*Δ*fliC*/pMMB*rocS1* (Fig. 3A, lane 2) could be observed. The only difference resulted in the presence of a band at an apparent molecular mass of about 130 kDa. The band was excised from the gel and subjected to MALDI-TOF mass spectrometry analysis. The results indicated that this band corresponded to the RocS1 protein, thus confirming that it was efficiently produced from pMMB*rocS1*. In a parallel but separate experiment, the proteins were further blotted onto nitrocellulose membranes and revealed with antibodies directed against CupC1 (see Materials and Methods). A band at an apparent molecular mass of 22 kDa, which corresponds to the mass of CupC1, could readily be detected in the sample from the *rocS1*-overexpressing strain (Fig. 3A, lane 4), which is lacking in the strain carrying the cloning vector pMMB67EH (Fig. 3A, lane 3). Our results showed that the overexpression of *rocS1*, which in turn induced *cupC* expression, finally resulted in the high-level production of the CupC1 fimbrial subunit. It was thus important to determine whether such production is concomitant with the surface assembly of CupC1-containing fibers.

CupC1 and CupB1 fimbrial subunits could be sheared off the bacterial cell surface. In order to proceed to the recovery of putative CupC fimbriae, we used the PAO1Δ*pilA*Δ*fliC* strain, which overproduced RocS1 (pMMB*rocS1*). In this case, the lack of type IV pili and flagella facilitates the analysis of the sheared extracellular appendages (see Materials and Methods). Briefly, the shearing procedure was conducted as follows. Bacteria were scraped from plates and resuspended in L broth. Appendages attached to the cell surface were sheared by gentle agitation and harvested by centrifugation. The supernatant was then subjected to AS precipitation and further designated as SFs. The protein content equivalent to a 0.25 OD_{600} unit of bacterial culture was loaded on SDS gels containing 12% acrylamide (Fig. 3B). The SDS gels were stained with Coomassie blue (Fig. 3B, lanes 1 to 3) or used to transfer proteins onto nitrocellulose membranes for immunodetection using antibodies directed against CupC1 (Fig. 3B, lanes 4 to 6). In the strain overproducing RocS1, we could detect a band whose molecular mass corresponded to that of the CupC1 protein (Fig. 3B, lanes 1 and 2). The identity of this protein was confirmed both by mass spectrometry and by immunoblotting using antibodies directed against CupC1 (Fig. 3B, lanes 4 and 5). CupC1 was

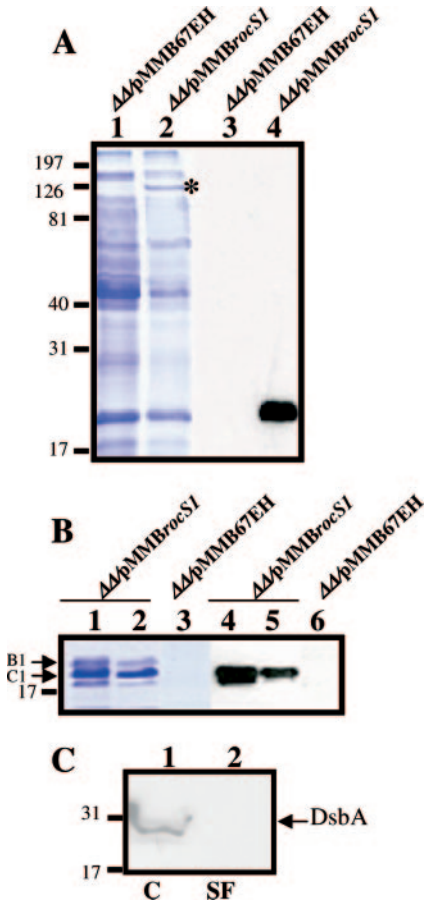

FIG. 3. Detection of the CupC1 subunit in whole cells and in sheared appendages. (A) Whole-cell extracts from the PAO1Δ*pilA*Δ*fliC* (ΔΔ) strain containing either pMMB67EH or pMMB*rocS1* were collected after 72 h of growth onto M63 plates supplemented with 0.4% L-arginine and 1 mM IPTG. The proteins were separated on 12% acrylamide–SDS gels stained with Coomassie blue (lanes 1 and 2) or transferred onto nitrocellulose and revealed with CupC1 antibodies (lanes 3 and 4). The position of the RocS1 band is indicated by an asterisk. Numbers on the left are molecular mass standards (kDa). (B) Production and detection of the CupC1 protein in SFs obtained from the bacterial cell surfaces of strains PAO1Δ*pilA*Δ*fliC*/pMMB*rocS1* (lanes 1, 2, 4, and 5) and PAO1Δ*pilA*Δ*fliC*/pMMB67EH (lanes 3 and 6). The proteins contained in the SFs were precipitated with 50% AS (lanes 1, 3, 4, and 6) and 55% AS (lanes 2 and 5). The CupB1 and the CupC1 proteins are indicated by the upper (B1) and the lower (C1) arrows. The Coomassie blue-stained gel corresponds to lanes 1 through 3, and the blot revealed with CupC1 antibodies corresponds to lanes 4 through 6. (C) The absence of intracellular proteins in the SFs was assessed by immunodetection of the DsbA periplasmic protein using appropriate antibody. C, whole-cell extracts.

not detectable in the *P. aeruginosa* strain transformed with the empty vector (Fig. 3B, lanes 3 and 6). These results indicated that detectable production of CupC1 resulted in its occurrence at the bacterial cell surface. We further checked that the protein content found in the SFs is not due to bacterial cell lysis. The OTCase protein (data not shown) and the periplasmic DsbA protein (Fig. 3C) were detected only in whole-cell extracts (Fig. 3C, lane 1) and not in the SFs (Fig. 3C, lane 2). This observation confirmed that we properly sheared the bacterial cell surface without any detectable leakage of intracellular proteins.

Interestingly, a band with a slightly higher molecular weight than that of CupC1 was also found abundantly in the SFs obtained from the RocS1-overproducing strain (Fig. 3B, lanes 1 and 2). Furthermore, this band was absent in the control strain containing the empty vector (Fig. 3B, lane 3). The molecular mass of this band suggested that it could correspond to CupB1. We were not successful in raising antibodies directed against CupB1, but mass spectrometry analysis confirmed that it corresponded to the CupB1 protein. Overall, our results showed that RocS1 overproduction resulted in the production of both the CupB1 and CupC1 proteins, but more interestingly, we showed that these proteins could be recovered from the cell surface, thus suggesting that they were assembled into fibers.

Specificity of CupB1 and CupC1 assembly. We investigated whether the exposition of the CupB1 and CupC1 fimbrial subunits at the bacterial cell surface required their respective usher components, CupB3 and CupC3, or whether these components are interchangeable. As previously described, we prepared extracellular appendages from the parental *P. aeruginosa* PAK strain and the isogenic PAK::*cupB3* and PAK::*cupC3* mutants (36), which overproduced RocS1 (pMMB*rocS1*) (Fig. 4A). Protein separation on SDS-PAGE coupled with MALDI-TOF mass spectrometry analysis allowed us to clearly detect the CupB1 protein in SFs obtained from the PAK (Fig. 4A, lane 1) and the PAK::*cupC3* (Fig. 4A, lane 3) strains but not from the PAK::*cupB3* strain (Fig. 4A, lane 2). In the same way, the CupC1 protein was present in the SFs at the surface of the wild-type strain (Fig. 4A, lane 1) and of the PAK::*cupB3* mutant (Fig. 4B, lane 2) but not at the surface of the PAK::*cupC3* mutant (Fig. 4B, lane 3). These results were confirmed by Western blot analysis using the CupC1 antibodies (data not shown). Our data suggest that assembly of CupB1 and CupC1 fimbrial subunits at the bacterial cell surface requires their respective CupB3 and CupC3 usher proteins.

In order to fully address the specificity of the assembly process, we engineered a *cupB3 cupC3* double-deletion mutant of the PAO1Δ*pilA*Δ*fliC* strain. We also constructed the isogenic *cupB3* and *cupC3* mutants for comparison. In all strains, we introduced the pMMB*rocS1* plasmid, and we tested the presence of CupC1 in the SFs of the mutants and the PAO1Δ*pilA*Δ*fliC* parental strain (Fig. 4B). Unlike with the parental strain (Fig. 4B, lanes 1 and 2), the CupC1 protein could not be immunodetected in the SFs of the *cupC3* mutant (Fig. 4B, lane 4). Importantly, CupC1 could be detected in the whole-cell extracts (Fig. 4B, lane 3) of this mutant, indicating that it is produced but not assembled. Introduction in *trans* of the *cupC3* gene (pBBR*cupC3*) in this mutant restored the recovery of CupC1 from SFs (Fig. 4B, lane 6). The presence of the CupC1 protein in the SFs obtained from the *cupB3* mutant

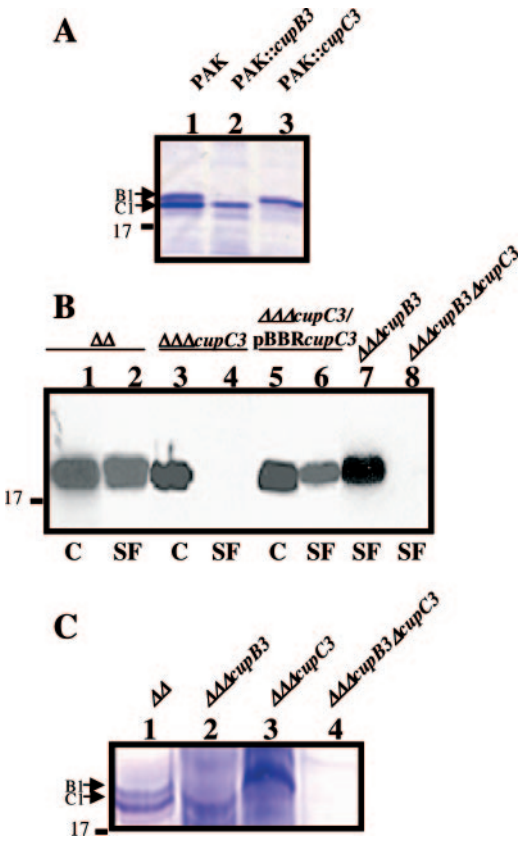

FIG. 4. Extracellular assembly of CupC1 and CupB1 proteins in a specific usher-dependent manner. (A) Protein samples obtained from SFs from the PAK, PAK::*cupB3*, and PAK::*cupC3* strains transformed with pMMB*rocS1*. Proteins contained in the SFs were precipitated with 50% AS, separated on SDS gels, and stained with Coomassie blue. The CupB1 and the CupC1 proteins are indicated by the upper (B1) and the lower (C1) arrows, respectively. (B) Detection of the CupC1 protein in whole-cell extracts (C) (lanes 1, 3, and 5) and in SFs (lanes 2, 4, 6, 7, and 8) of PAO1Δ*pilA*Δ*fliC* (ΔΔ), PAO1Δ*pilA*Δ*fliC*Δ*cupC3* (ΔΔΔ*cupC3*), PAO1Δ*pilA*Δ*fliC*Δ*cupC3*/pBBR*cupC3* (ΔΔΔ*cupC3*/pBBR*cupC3*), PAO1Δ*pilA*Δ*fliC*Δ*cupB3* (ΔΔΔ*cupB3*), and PAO1Δ*pilA*Δ*fliC*Δ*cupB3*Δ*cupC3* (ΔΔΔ*cupB3*Δ*cupC3*). All strains contained the pMMB*rocS1* plasmid. (C) Coomassie blue staining of proteins contained in SFs from PAO1Δ*pilA*Δ*fliC* (ΔΔ, lane 1), PAO1Δ*pilA*Δ*fliC*Δ*cupB3* (ΔΔΔ*cupB3*, lane 2), PAO1Δ*pilA*Δ*fliC*Δ*cupC3* (ΔΔΔ*cupC3*, lane 3), and PAO1Δ*pilA*Δ*fliC*Δ*cupB3*Δ*cupC3* (ΔΔΔ*cupB3*Δ*cupC3*, lane 4). All strains contained pMMB*rocS1*. The CupB1 and the CupC1 proteins are identified by the upper (B1) and the lower (C1) arrows, respectively.

(Fig. 4B, lane 7) but its absence in the corresponding preparation from the *cupB3 cupC3* double mutant (Fig. 4B, lane 8) further confirmed that CupC fimbrial assembly at the bacterial cell surface occurred specifically through the CupC3 usher protein. The CupB1 protein (Fig. 4C) was no longer recovered in the SFs obtained from the *cupB3* mutant (Fig. 4C, lane 2) and from the *cupB3 cupC3* double mutant (Fig. 4C, lane 4), as seen by analysis of Coomassie blue-stained gels. However, CupB1 was present in the SF obtained from the *cupC3* mutant (Fig. 4C, lane 3), from the parental strain (Fig. 4C, lane 1), and from the *cupB3 cupC3* mutant *trans*-complemented with the *cupB3* gene (data not shown). These results confirmed that the assembly of CupB1 and CupC1 fimbrial subunits occurs

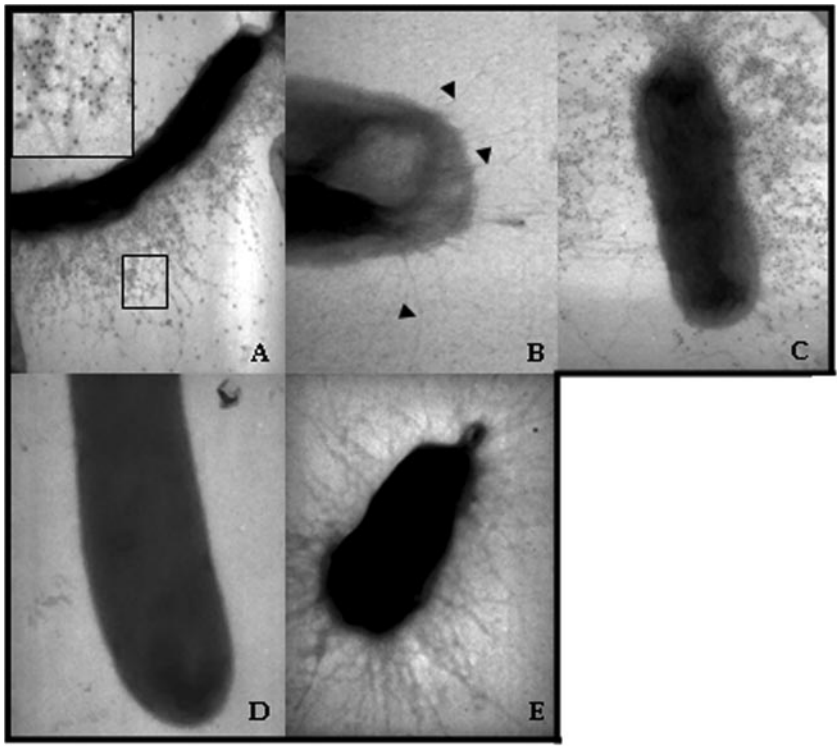

FIG. 5. Images of CupB and CupC appendages at the *P. aeruginosa* cell surface. Long fimbriae decorated with gold particles coupled to specific antibodies directed against CupC1 were peritrichously distributed at the cell surface of the PAO1Δ*pilA*Δ*fliC* strain (A), in which RocS1 was overproduced (pMMB*rocS1*) (inset in upper left-hand corner, ×20,000 magnification of central boxed area). The CupC1-labeled fimbriae were absent in the mutant PAO1Δ*pilA*Δ*fliC*Δ*cupC3*/pMMB*rocS1* (magnification, ×50,000) (B) but recovered when the *cupC3* mutation was *trans*-complemented with the *cupC3* gene (magnification, ×20,000) (C). The unlabeled CupB fimbriae were visualized (arrowheads) in the *cupC3* mutant (B) and absent in the PAO1Δ*pilA*Δ*fliC*Δ*cupB3*Δ*cupC3* mutant (D) (magnification, ×50,000) but recovered when the *cupB3* mutation was *trans*-complemented with the *cupB3* gene (magnification, ×20,000) (E).

specifically through their respective CupB3 and CupC3 usher proteins.

Overall, our results demonstrate that assembly of Cup fimbrial subunits can only occur through a dedicated outer membrane usher protein and that CupB3 and CupC3 cannot be exchanged. In redundant systems, such as the Pap and the Fim fimbrial systems of *E. coli*, the usher protein, which forms an oligomeric channel in the outer membrane (33), is also known for playing a central role in determining the specificity toward the chaperone–fimbrial-subunit complex (6). The PapDG chaperone-adhesin complex cannot bind the FimD usher (29), and the FimCH chaperone-adhesin complex cannot bind the PapC usher (29). The molecular characterization of the PapC usher clearly revealed that the N-terminal domain is required for initial binding, specifically the Pap chaperone–fimbrial-subunit complexes (24), whereas the C-terminal domain is required in the subsequent assembly steps (34). However, a C-terminally truncated PapC (PapC*) is still able to bind Pap chaperone–fimbrial-subunit complexes, and assembly of P pili can occur through a PapC*-FimD hetero-oligomeric complex (34).

Visualization of the CupB and CupC fimbriae. We looked further at the presence of CupB and CupC fimbriae on the surface of the PAO1Δ*pilA*Δ*fliC* strain, in which RocS1 was overproduced, by using electron microscopy coupled with immunogold labeling using anti-CupC1 antibodies or by negative staining (see Materials and Methods). Long fimbriae decorated with gold particles coupled to CupC1 antibodies (Fig. 5) were observed at the bacterial cell surface of the RocS1-overproducing strain (Fig. 5A) but were not identified in the PAO1Δ*pilA*Δ*fliC* strain that was transformed with the vector pMMB67EH (data not shown). The CupC1-containing fimbriae were peritrichously distributed (Fig. 5A) at the surface of the bacterial cell envelope. This CupC fimbrial distribution in the PAO1Δ*pilA*Δ*fliC* strain was found to be independent of the presence of other appendages by comparing it with a PAO1Δ*pilA* mutant or a PAO1Δ*fliC* mutant (data not shown). We further observed that no CupC1-containing fimbriae were assembled at the surface of the *cupC3* mutant (Fig. 5B), whereas CupC1 fimbrial assembly was restored when the mutant was *trans*-complemented with the *cupC3* gene (Fig. 5C), thus confirming that CupC1 assembly into fibers is dependent on the usher protein CupC3. Since we have no CupB1-related antibodies, we were unable to specifically detect CupB fimbriae. However, a careful examination of images obtained with the *cupC3* mutant (Fig. 5B) indicated that non-CupC1-labeled fibrils radiate outwards from the bacterial cell surface. These fibrils were no longer observed in a *cupB3 cupC3* mutant (Fig. 5D), but their presence was restored in the *cupB3 cupC3* mutant *trans*-complemented with the *cupB3* gene (Fig. 5E).

The final architecture of fibrous organelles assembled by chaperone-usher pathways has been classified as having rigid

pili and thin fibrillae on the one hand and afimbrial and capsular material on the other (30). Although rigid pili and thin fibrillae are made from several different subunits, the nonpilus material is composed of only one or sometimes two different subunits and does not contain any specialized adhesin, even though it confers adhesive properties. Moreover, structures assembled by the FGS chaperone-usher subfamily are rigid pili or thin fibrillae, whereas structures assembled by the FGL chaperone-usher subfamily are nonfiber organelles forming afimbrial adhesive structures at the surfaces of the bacteria (15). The cluster corresponding to the CupC machinery is restricted to three genes encoding one fimbrial subunit, one chaperone, and one usher protein. Even though the CupC system involved only one fimbrial subunit, the classification of the CupC2 chaperone protein in the FGS subfamily suggested that it would be implicated in the assembly of homopolymeric fimbriae rather than of capsule-like material. Our data obtained by electron microscopy coupled with CupC1 immunodetection allowed us to clearly identify homopolymeric fimbriae assembled at the surfaces of *P. aeruginosa* cells. The CupC1 fimbrial distribution resembles the peritrichous distribution of Pef pili assembled by the *pef* operon in *Salmonella enterica* serovar Typhimurium (1), fimbriae encoded by the *hifABCDE* operon of nonencapsulated *Haemophilus influenzae* (10), type 1 pili from uropathogenic strains of *E. coli* (14), SMF-1 fimbriae from *Stenotrophomonas maltophilia* (5), and type 3 fimbriae originally described to occur in *Klebsiella* species and identified as widely expressed in the *Enterobacteriaceae* family (11).

Conclusions. The *P. aeruginosa* PAO1 genome sequence (31) revealed the presence of a family of orthologues (*cup*) to genes encoding proteins involved in the chaperone-usher pathway described to occur in *E. coli* (36). The *cup* genes appeared poorly expressed in a variety of media and under a variety of conditions. However, recent advances in the understanding of *P. aeruginosa* regulatory networks involved in the control of these *cup* genes have been made (20, 37, 38). A negative regulator, MvaT, which strongly represses *cupA* gene expression but has a much smaller effect on *cupB* and *cupC* gene expression, has been described (37). *cupB* and *cupC* gene expression was also recently described as being regulated by two members of the two-component regulatory systems named Roc1 and Roc2 (20). These systems control the expression of genes according to the environmental conditions and have allowed detection of the production of the CupB1 and CupC1 proteins. The present work further reveals for the first time that CupB1 and CupC1 are subunits assembled into fimbriae by a chaperone-usher pathway in *P. aeruginosa*. The CupB and CupC machineries, which belong to the FGS subfamily, assemble thin fimbriae widely distributed at the bacterial cell surface. Since the CupC machinery is encoded by a three-gene operon, the assembly of CupC fimbriae probably results from the homopolymerization of the CupC1 protein in fibers devoid of adhesin at their tips. In the case of the CupB fimbriae, it is likely that they are heteropolymeric fibers of the CupB1 protein with the putative CupB6 adhesin located at their tips. CupB and CupC fimbrial assembly at the *P. aeruginosa* cell surface occurs strictly through their dedicated outer membrane usher proteins, and the resulting CupB and CupC fimbriae cooperate in cell-cell interactions and microcolony formation during the biofilm maturation process. The redundancy of the chaperone-usher systems in the *P. aeruginosa* genome, combined with a complex regulatory network tightly controlling their expression, highlights the diversity of organelles that the bacterium can expose at its surface while encountering different environments or supports. However, particular traits of each fimbrial structure may determine a specific function for the colonization of an ecological niche and may confer tissue-specific adhesive properties (23, 30).

ACKNOWLEDGMENTS

We thank A. Bernadac, I. Ventre, G. Ball, and D. Moinier for technical assistance and A. Fox and I. Vallet-Gely for their helpful comments. We also thank D. Haas (Université de Lausanne, Switzerland) for the gift of a specific rabbit polyclonal antibody directed against the OTCase protein and K. E. Jaeger (IMET, Jülich, Germany) for the gift of a specific rabbit polyclonal antibody directed against the periplasmic thiol-disulfide interchange protein (DsbA). We thank S. Lory (Harvard University, Boston, MA) for providing pMMB*rocS1*.

A.F. and S.D.B.'s work is supported by the French Cystic Fibrosis Foundation (VLM), the Bettencourt-Schueller Foundation, and CNRS institutional grants. S.R. is supported by the French Research and Technology Ministry. S.S. was supported by Marie Curie Fellowship EIF 502287 and the CNRS.

REFERENCES

1. **Bäumler, A. J., R. M. Tsolis, F. A. Bowe, J. G. Kuster, S. Hoffmann, and F. Heffron.** 1996. The *pef* fimbrial operon of *Salmonella typhimurium* mediates adhesion to murine small intestine and is necessary for fluid accumulation in the infant mouse. Infect. Immun. **64:**61–68.
2. **Choudhury, D., A. Thompson, V. Stojanoff, S. Langermann, J. Pinker, S. J. Hultgren, and S. D. Knight.** 1999. X-ray structure of the FimC-FimH chaperone-adhesin complex from uropathogenic *Escherichia coli*. Science **285:** 1061–1066.
3. **D'Argenio, D. A., M. W. Calfee, P. B. Rainey, and E. C. Pesci.** 2002. Autolysis and autoaggregation in *Pseudomonas aeruginosa* colony morphology mutants. J. Bacteriol. **184:**6481–6489.
4. **de Bentzmann, S., M. Aurouze, G. Ball, and A. Filloux.** 2006. FppA, a novel *Pseudomonas aeruginosa* prepilin peptidase involved in assembly of type IVb pili. J. Bacteriol. **188:**4851–4860.
5. **de Oliveira-Garcia, D., M. Dall'Agnol, M. Rosales, A. C. Azzuz, N. Alcantara, M. B. Martinez, and J. A. Giron.** 2003. Fimbriae and adherence of *Stenotrophomonas maltophilia* to epithelial cells and to abiotic surfaces. Cell. Microbiol. **5:**625–636.
6. **Dodson, K. W., F. Jacob-Dubuisson, R. T. Striker, and S. J. Hultgren.** 1993. Outer-membrane PapC molecular usher discriminately recognizes periplasmic chaperone-pilus subunit complexes. Proc. Natl. Acad. Sci. USA **90:**3670–3674.
7. **Dodson, K. W., J. S. Pinkner, T. Rose, G. Magnusson, S. J. Hultgren, and G. Waksman.** 2001. Structural basis of the interaction of the pyelonephritic *E. coli* adhesin to its human kidney receptor. Cell **105:**733–743.
8. **Filloux, A., S. de Bentzmann, M. Aurouze, A. Lazdunski, and I. Vallet.** 2004. Fimbrial genes in *Pseudomonas aeruginosa* and *Pseudomonas putida*, p. 721–748. *In* J.-L. Ramos (ed.), *Pseudomonas*. Kluwer Academic, New York, NY.
9. **Galyov, E. E., A. V. Karlishev, T. V. Chernovskaya, D. A. Dolgikh, O. Y. Smirnov, K. I. Volkovoy, V. M. Abramov, and V. P. Zav'yalov.** 1991. Expression of the envelope antigen F1 of *Yersinia pestis* is mediated by the product of *caf1M* gene having homology with the chaperone protein PapD of *Escherichia coli*. FEBS Lett. **286:**79–82.
10. **Geluk, F., P. P. Eijk, S. M. van Ham, H. M. Jansen, and L. van Alphen.** 1998. The fimbria gene cluster of nonencapsulated *Haemophilus influenzae*. Infect. Immun. **66:**406–417.
11. **Gerlach, G. F., B. L. Allen, and S. Clegg.** 1989. Type 3 fimbriae among enterobacteria and the ability of spermidine to inhibit MR/K hemagglutination. Infect. Immun. **57:**219–224.
12. **Haußler, S.** 2004. Biofilm formation by the small colony variant phenotype of *Pseudomonas aeruginosa*. Environ. Microbiol. **6:**546–551.
13. **Hot, D., R. Antoine, G. Renauld-Mongenie, V. Caro, B. Hennuy, E. Levillain, L. Huot, G. Wittmann, D. Poncet, F. Jacob-Dubuisson, C. Guyard, F. Rimlinger, L. Aujame, E. Godfroid, N. Guiso, M. J. Quentin-Millet, Y. Lemoine, and C. Locht.** 2003. Differential modulation of *Bordetella pertussis* virulence genes as evidenced by DNA microarray analysis. Mol. Genet. Genomics **269:**475–486.
14. **Hull, R. A., R. E. Gill, P. Hsu, B. H. Minshew, and S. Falkow.** 1981. Con-

struction and expression of recombinant plasmids encoding type 1 or D-mannose-resistant pili from a urinary tract infection *Escherichia coli* isolate. Infect. Immun. **33:**933–938.
15. **Hung, D. L., S. D. Knight, R. M. Woods, J. S. Pinkner, and S. J. Hultgren.** 1996. Molecular basis of two subfamilies of immunoglobulin-like chaperones. EMBO J. **15:**3792–3805.
16. **Jones, C. H., J. S. Pinkner, R. Roth, J. Heuser, A. V. Nicholes, S. N. Abraham, and S. J. Hultgren.** 1995. FimH adhesin of type 1 pili is assembled into a fibrillar tip structure in the Enterobacteriaceae. Proc. Natl. Acad. Sci. USA **92:**2081–2085.
17. **Kaniga, K., I. Delor, and G. R. Cornelis.** 1991. A wide-host-range suicide vector for improving reverse genetics in gram-negative bacteria: inactivation of the *blaA* gene of *Yersinia enterocolitica*. Gene **109:**137–141.
18. **Kar, S., S. C.-M. To, and C. C. Brinton, Jr.** 1990. Cloning and expression in *Escherichia coli* of LKP pilus genes from a nontypeable *Haemophilus influenzae* strain. Infect. Immun. **58:**903–908.
19. **Klausen, M., A. Heydorn, P. Ragas, L. Lambertsen, A. Aaes-Jorgensen, S. Molin, and T. Tolker-Nielsen.** 2003. Biofilm formation by *Pseudomonas aeruginosa* wild type, flagella and type IV pili mutants. Mol. Microbiol. **48:**1511–1524.
20. **Kulasekara, H. D., I. Ventre, B. R. Kulasekara, A. Lazdunski, A. Filloux, and S. Lory.** 2005. A novel two-component system controls the expression of *Pseudomonas aeruginosa* fimbrial *cup* genes. Mol. Microbiol. **55:**368–380.
21. **Labaer, J., Q. Qiu, A. Anumanthan, W. Mar, D. Zuo, T. V. Murthy, H. Taycher, A. Halleck, E. Hainsworth, S. Lory, and L. Brizuela.** 2004. The *Pseudomonas aeruginosa* PAO1 gene collection. Genome Res. **14:**2190–2200.
22. **Lund, B., F. Lindberg, B. I. Marklund, and S. Normark.** 1987. The PapG protein is the alpha-D-galactopyranosyl-(1→4)-beta-D-galactopyranose-binding adhesin of uropathogenic *Escherichia coli*. Proc. Natl. Acad. Sci. USA **84:**5898–5902.
23. **Marklund, B. I., J. M. Tennent, E. Garcia, A. Hamers, M. Baga, F. Lindberg, W. Gaastra, and S. Normark.** 1992. Horizontal gene transfer of the *Escherichia coli pap* and *prs* pili operons as a mechanism for the development of tissue-specific adhesive properties. Mol. Microbiol. **6:**2225–2242.
24. **Ng, T. W., L. Akman, M. Osisami, and D. G. Thanassi.** 2004. The usher N terminus is the initial targeting site for chaperone-subunit complexes and participates in subsequent pilus biogenesis events. J. Bacteriol. **186:**5321–5331.
25. **O'Toole, G. A., and R. Kolter.** 1998. Flagellar and twitching motility are necessary for *Pseudomonas aeruginosa* biofilm development. Mol. Microbiol. **30:**295–304.
26. **Prugnola, A., B. Arico, R. Manetti, R. Rappuoli, and V. Scarlato.** 1995. Response of the *bvg* regulon of *Bordetella pertussis* to different temperatures and short-term temperature shifts. Microbiology **141:**2529–2534.
27. **Sauer, F. G., J. S. Pinkner, G. Waksman, and S. J. Hultgren.** 2002. Chaperone priming of pilus subunits facilitates a topological transition that drives fiber formation. Cell **111:**543–551.
28. **Sauer, F. G., H. Remaut, S. J. Hultgren, and G. Waksman.** 2004. Fiber assembly by the chaperone-usher pathway. Biochim. Biophys. Acta **1694:**259–267.
29. **Saulino, E. T., D. G. Thanassi, J. S. Pinkner, and S. J. Hultgren.** 1998. Ramifications of kinetic partitioning on usher-mediated pilus biogenesis. EMBO J. **17:**2177–2185.
30. **Soto, G. E., and S. J. Hultgren.** 1999. Bacterial adhesins: common themes and variations in architecture and assembly. J. Bacteriol. **181:**1059–1071.
31. **Stover, C. K., X. Q. Pham, A. L. Erwin, S. D. Mizoguchi, P. Warrener, M. J. Hickey, F. S. Brinkman, W. O. Hufnagle, D. J. Kowalik, M. Lagrou, R. L. Garber, L. Goltry, E. Tolentino, S. Westbrock-Wadman, Y. Yuan, L. L. Brody, S. N. Coulter, K. R. Folger, A. K. Kas, K. Larbig, R. Lim, K. Smith, D. Spencer, G. K. Wong, Z. Wu, I. T. Paulsen, J. Reizer, M. H. Saier, R. E. Hancock, S. Lory, and M. V. Olson.** 2000. Complete genome sequence of *Pseudomonas aeruginosa* PAO1, an opportunistic pathogen. Nature **406:**959–964.
32. **Thanassi, D. G., E. T. Saulino, and S. J. Hultgren.** 1998. The chaperone/usher pathway: a major terminal branch of the general secretory pathway. Curr. Opin. Microbiol. **1:**223–231.
33. **Thanassi, D. G., E. T. Saulino, M. J. Lombardo, R. Roth, J. Heuser, and S. J. Hultgren.** 1998. The PapC usher forms an oligomeric channel: implications for pilus biogenesis across the outer membrane. Proc. Natl. Acad. Sci. USA **95:**3146–3151.
34. **Thanassi, D. G., C. Stathopoulos, K. Dodson, D. Geiger, and S. J. Hultgren.** 2002. Bacterial outer membrane ushers contain distinct targeting and assembly domains for pilus biogenesis. J. Bacteriol. **184:**6260–6269.
35. **Thanassi, D. G., C. Stathopoulos, A. Karkal, and H. Li.** 2005. Protein secretion in the absence of ATP: the autotransporter, two-partner secretion and chaperone/usher pathways of gram-negative bacteria. Mol. Membr. Biol. **22:**63–72.
36. **Vallet, I., J. W. Olson, S. Lory, A. Lazdunski, and A. Filloux.** 2001. The chaperone/usher pathway of *Pseudomonas aeruginosa*: identification of fimbrial gene clusters (*cup*) and their involvement in biofilm formation. Proc. Natl. Acad. Sci. USA **98:**6911–6916.
37. **Vallet, I., S. P. Diggle, R. E. Stacey, M. Cámara, I. Ventre, S. Lory, A. Lazdunski, P. Williams, and A. Filloux.** 2004. Biofilm formation in *Pseudomonas aeruginosa*: fimbrial *cup* gene clusters are controlled by the transcriptional regulator MvaT. J. Bacteriol. **186:**2880–2890.
38. **Vallet-Gely, I., K. E. Donovan, R. Fang, J. K. Joung, and S. L. Dove.** 2005. Repression of phase-variable *cup* gene expression by H-NS-like proteins in *Pseudomonas aeruginosa*. Proc. Natl. Acad. Sci. USA **102:**11082–11087.
39. **Williams, C. L., P. E. Boucher, S. Stibitz, and P. A. Cotter.** 2005. BvgA functions as both an activator and a repressor to control Bvg phase expression of *bipA* in *Bordetella pertussis*. Mol. Microbiol. **56:**175–188.